The Cryosphere Discuss., 8, 1305–1336, 2014
www.the-cryosphere-discuss.net/8/1305/2014/
doi:10.5194/tcd-8-1305-2014

The Cryosphere Discussions
Open Access

Climatic and topographic influences on glacier distribution in the Bhutan Himalaya

H. Nagai[1], **K. Fujita**[1], **A. Sakai**[1], **T. Nuimura**[1], **and T. Tadono**[2]

[1]Graduate School of Environmental Studies, Nagoya University, Nagoya, Japan
[2]Earth Observation Research Center, Japan Aerospace Exploration Agency, Tsukuba, Japan

Received: 21 January 2014 – Accepted: 10 February 2014 – Published: 25 February 2014

Correspondence to: H. Nagai (hirotonagai@nagoya-u.jp)

Published by Copernicus Publications on behalf of the European Geosciences Union.

Abstract

The locations and extent of mountain glaciers are affected by climatic constraints such as air temperature, precipitation, and solar radiation, as well as by local topography, which influences avalanche accumulation and debris supply. To evaluate these influences on the elevational distribution of glaciers in the Bhutan Himalaya, we created a glacier inventory together with debris-covered area and potential material-supply (PMS) slopes using satellite images with high spatial resolution. The median elevation of a glacier, which is used as a proxy of the equilibrium line altitude (ELA), decreases with increasing annual precipitation, suggesting the influence of climatic factors, according to which the ELA is lowered in relatively warm and humid environments, and raised when the opposite conditions prevail. We found a weak but significant influence of topography on the elevational distribution of glaciers, indicated by the relationship between the deviation of the median elevation of an individual glacier from the regional average and the PMS slope ratio (defined as the ratio of the PMS slope area to glacier area). We further analysed the dependency of the median glacier elevation on the gradient and aspect of PMS slopes. We found that the median elevation is affected by the avalanche-driven redistribution of snow accumulation on debris-free glaciers, and that in debris-covered glaciers the debris supply affects glacier extent through the insulation effect of the debris layer.

1 Introduction

Glaciers are key indicators of climate change (e.g., Kaser et al., 2006; Bolch et al., 2012), and glacial meltwater is an important water resource for human consumption and agriculture in arid regions (e.g., Immerzeel et al., 2010; Kaser et al., 2010). The contribution of glacier mass loss to global sea-level rise is also a current societal concern (e.g., Raper and Braithwaite, 2006; Radić and Hock, 2011). In the high mountains of Asia, which contain the largest number of glaciers outside the polar regions, spatially heterogeneous shrinkage of glaciers has been identified by in situ measurements (Yao et al., 2012), remote sensing approaches (Kääb et al., 2012; Gardelle et al., 2013), and model simulations (Fujita and Nuimura, 2011). A few studies provided precise hypsometries (area–altitude distribution) of glaciers in the Himalayas (Bolch et al., 2012; Basnett et al., 2013), which are important basses for projecting the influence of glacier changes on meltwater discharge. In particular, glaciers in humid monsoonal climates, such as those in the Bhutan Himalaya, are expected to be highly sensitive to changing climate (Fujita, 2008; Fujita and Nuimura, 2011). However, the elevational and spatial distribution of glaciers and their relationships with climate and topography in the Bhutan Himalaya are largely unknown, as neither observational evidence nor the present locations of glaciers are available for this area, with the exception of a preliminary report using remote sensing data (Karma et al., 2003).

In terms of climatic influences on glaciers, it has been revealed that the relationship between climatic regimes and equilibrium line altitudes (ELAs) can be expressed by a polynomial equation consisting of summer mean temperature and annual precipitation (Ohmura et al., 1992). Larger snow accumulations are related to lowered glacier ELAs, and thus the presence of glaciers in warmer environments, and vice versa. Although ELAs are obtainable only by direct measurements of mass balance or other estimations, such as the use of accumulation–area ratio methods, few data are available for glaciers in the Bhutan Himalaya. For such region, the median elevation, which divides the glacier area in half, as a proxy for the ELA for unmeasured glaciers, can be adopted as proposed by Braithwaite and Raper (2009).

One of the most concerning features of Himalayan glaciers is the extent of debris cover, which potentially prevents ice melting if the debris layer is sufficiently thick (Mattson et al., 1993), and which stabilizes their termini surrounded by their equivocal boundary (Scherler et al., 2011a). In terms of glacier hypsometry and median elevation, a massive debris mantle can decrease the melting rate of ice, and possibly enhance the expansion of debris-covered ablation areas, thus lowering the median elevation. Topographic influences on the extent of glaciers are related to debris supply, which appears to correlate highly with slope gradients above glaciers in the Himalaya (Scherler et al., 2011b) or with the extent of southwest-facing slopes above glaciers in the Bhutan Himalaya (Nagai et al., 2013). Avalanche-fed accumulation is also another influence of topography on the extent of glaciers (Hewitt, 2011). Redistribution of snow accumulation by avalanches can possibly increase the size of the ablation area at lower elevations through increased ice flux, thus resulting in a lowering of the median elevation. However, influences of these two factors on elevation distribution of glacier are not well understood.

Some previous studies have reported on the spatial distribution of precipitation (Eguchi, 1991), changes in terminus locations of glaciers (Karma et al., 2003), topographic asymmetries affecting dynamic regimes (Kääb, 2005), and the formation of debris-covered areas (Nagai et al., 2013) in relation to glaciers in the Bhutan Himalaya. However, it is not yet known which factors are different between the debris-free and debris-covered nature of glacial termini, and which factors control glacier extent, particularly in terms of elevation. In this study, we aim to understand the influences of climate and topography on the elevational distribution of glaciers in the Bhutan Himalaya, a region in which drastic precipitation gradients occur over a narrow latitudinal range ($< 1^{\circ}$). We mainly analysed the median elevations of glaciers (as an ELA proxy) in relation to precipitation (a climatic variable) and the slopes situated above a glacier (a topographic variable).

2 Data and methods

2.1 Study site and datasets

We focused on a latitude–longitude domain in the Bhutan Himalaya (27°36′–28°30′N, 89°12′–92°00′E) in which glaciers are located at an elevational range of 4000–7500 m a.s.l. Satellite-derived glacier inventories for this domain have been released by the International Centre for Integrated Mountain Development (Mool et al., 2001), Global Land Ice Measurements from Space (Raup and Khalsa, 2007), and the Randolph Consortium (Arendt et al., 2012; Pfeffer et al., 2014). It has been pointed out, however, that seasonal snow cover and debris cover resulted in misinterpretation of glacier outlines. In addition, the outlines including mountain terrains and rock glaciers, omission of many glaciers, and highly generalized glaciers were reported. Wrong geolocation such as systematic shift causes serious errors on glacier distribution (Pfeffer et al., 2014). In the Bhutan Himalaya, for instance, it would be difficult for small glaciers and heavily debris-covered glaciers distributed in the southern part of the country to be correctly delineated because of the complex topography and the fact that many images are affected by snow cover, which make the identification of glacier boundaries equivocal. Therefore, we generated a new glacier inventory based on manual delineation of glaciers, using advanced satellite imagery with high spatial resolution.

In addition to delineation of the glacier itself, debris-covered areas and potential material-supply (PMS) slopes were separately delineated so as to facilitate the analysis of topographical influences on glacier distribution. We defined debris-covered areas as zones where ice cannot be seen on account of debris mantles in glacier ablation zones, but which does not include dirty glacier ice. A PMS slope is defined as a mountain surface from which any supply of snow, ice, or debris to the glacier can be expected. The PMS slopes are equivalent to the "potential debris-supply slopes" of Nagai et al. (2013), which were as potential sources of debris mantles and contributions to the formation of debris-covered areas on glaciers. However, in this study, we renamed the index so as to also take into account the accumulation of snow and ice by avalanches.

For glacier delineation, we used 58 scenes of the Panchromatic Remote-sensing Instrument for Stereo Mapping (PRISM) on board the Advanced Land Observing Satellite (ALOS). They were acquired repeatedly between 2007 and 2011 within the ALOS orbit paths of 154–158 (latitudinal location), and the frames of 3030–3045 (longitudinal location) (Table S3). The spatial resolution of the images is 2.5 m, and they are orthorectified with a PRISM-derived digital surface model using Ortho-image Generation Software for ALOS PRISM (Tadono et al., 2012). If multiple images were available for an area, we selected the image with the least snow cover for glacier identification. If no preferred PRISM image was available in a given area, we used 10 m resolution composite colour images from the Advanced Visible and Near Infrared Radiometer type 2 (AVNIR2) on board ALOS (Table S4). These images. which were acquired in the same period and location of the PRISM images, are orthorectified by a digital elevation model derived from the Shuttle Radar Topography Mission (SRTM DEM).

To generate 20 m contour lines, which were used to separate glacier connections at accumulation zones and to delineate PMS slopes, we utilized the second version of the Global Digital Elevation Model generated from the Advanced Spaceborne Thermal Emission and Reflection radiometer (ASTER GDEM2) provided by the National Aeronautics and Space Administration, United States, and the Ministry of Economy, Trade, and Industry, Japan. The images were synthesized from multiple ASTER images, with grid cell resolutions of 1 arc second (~ 30 m) (Tachikawa et al., 2011). Hayakawa et al. (2008) reported that accuracy of ASTER GDEM2 was better than that of SRTM DEM in steep terrain because of its higher resolution, fewer missing data, and better topographic representation, whereas the ASTER GDEM2 had large uncertainty on steep terrain, water or snow surfaces because of the lack of clear features (Toutin, 2002; Fujita et al., 2008). Therefore we utilized the GDEM2 to analyse distributions of elevations and aspects of surrounding slopes rather than snow-covered glacier surfaces. The outline polygons of features were overlain on bird's-eye view images in Google Earth™ to check delineation quality.

Tropical Rainfall Measuring Mission (TRMM) data were utilized to analyse spatial distributions of precipitation. We calculated annual precipitation between 1998 and 2012 from the TRMM 3B43 monthly product, at a spatial resolution of 0.25° (~ 25 km) (Huffman et al., 2007). In terms of accuracy in high mountains, monthly mean precipitation of the TRMM data showed better consistency with an in-situ measurement in the Nepal Himalaya than the other precipitation products (Yamamoto et al., 2011).

2.2 Definition used for delineation

Our method for generating the glacier inventory in the Bhutan Himalaya follows the visual interpretation and manual delineation method described by Nagai et al. (2013), in which the standard definition of glacier outlines is based on Raup and Khalsa (2007) and Rastner et al. (2012). PRISM images enable detailed identifications of (1) glaciers smaller than 100 m in length, (2) thermokarst features in debris-covered areas, and (3) surface features of unstable steep slopes around glaciers, from which material supply is potentially expected. The GDEM2-derived contour lines were layered on the PRISM images or the AVNIR2 images, and the Google Earth™ images of the same location were displayed on another panel. Visual interpretations and manual delineations were then conducted for glacier bodies, debris-covered areas, and PMS slopes, based on the procedures described below. The manual delineation of mountain glaciers with high-resolution satellite images causes high variability of outlines among different analysts, especially in debris-covered termini (Paul et al., 2013). Delineation work in this study was performed by one interpreter (the first author) and the outlines were modified three times by himself after a quality check by another interpreter.

First, each glacier terminus was identified, and contiguous ice bodies in all tributaries were delineated. Isolated ice bodies were defined as belonging to a downstream host glacier if their locations were proximal to the host glacier, and if they were expected to share ice transport processes with the host glacier. Smooth ice surface, crevasses around ice falls, and bergschrunds support the identification of glacier bodies, and allow us to exclude neighbouring snow-covered bedrock. Snow-covered accumulation zones continuously connecting some glaciers were separated along ridge lines, as interpreted from GDEM2-derived contours.

Because surface reflectance of debris-covered areas is similar to that of surrounding bedrock and/or moraines, we did not adopt automatic delineation methods. Instead, we visually interpreted surface features of debris-covered areas that were characterized by thermokarst features such as rugged small-relief supra-glacial ponds and ice cliffs

(Iwata et al., 2000). The upper boundary of debris cover often varied in several PRISM images taken on different dates. In such cases, the outline of the maximum area was adopted, taking temporary snow cover into account.

Continuous slopes between glacier margins and mountain ridges were delineated as PMS slopes if they tilted towards the glacier. Avalanche- or rockfall-induced scars and traces were taken as evidence of slope instability. Slopes intercepted by hills or lateral moraines, which would prevent avalanche or rockfall supply to a glacier, were excluded from the PMS slopes. Slopes of lateral and terminal moraines were included as long as they were inclined towards the glacier surface. These detailed surface features can be identified on PRISM images, although they are not fully expressed by contour lines.

3 Results

We delineated a total of 1579 glaciers in the Bhutan Himalaya (Table S1), distributed along the main E–W trending Himalayan range and along smaller branches extending in various directions (Fig. 1). The glaciers consist of 213 debris-covered glaciers and 1366 debris-free glaciers. While the number of debris-covered glaciers is smaller than that of debris-free glaciers, the total area of the former (1037.3 km^2) is much larger than that of the latter (570.2 km^2): on average, debris-covered glaciers are ten times larger than debris-free glaciers (4.87 km^2 vs. 0.42 km^2) (Table 1).

The total area of PMS slopes surrounding debris-covered glaciers (908.8 km^2) is 4.5 times greater than that surrounding debris-free glaciers (194.1 km^2), and the mean area of the PMS slopes for debris-covered glaciers is 30.5 times greater than that for debris-free glaciers (Table 1). We defined a PMS slope ratio parameter (PMS slope area divided by glacier area) to examine differences in the areas of PMS slopes as compared with the areas of debris-covered and debris-free glaciers. The mean PMS slope ratio for debris-covered glaciers (1.05) is two times greater than that for debris-free glaciers (0.47) (Table 1). The PMS slope area is highly correlated with debris-covered area, and PMS slopes are therefore considered to be the main sources of debris on glacier debris mantles in the Bhutan Himalaya (Nagai et al., 2013). The greater area of PMS slopes and the larger PMS ratios of debris-covered glaciers also suggest that PMS slopes are the main constraint on the extent to which a glacier is covered by debris.

Hypsometries (area–altitude distributions) of debris-covered and debris-free glaciers show that the maximum glacier area occurs at 5400 m a.s.l. for both glacier types (Fig. 2). The debris-covered glaciers are distributed over broader elevational ranges (4000–7500 m a.s.l.) than are debris-free glaciers (4800–6800 m a.s.l.) Mean median elevations of individual glaciers are 5537 ± 355 m a.s.l. for debris-covered glaciers and 5495 ± 285 m a.s.l. for debris-free glaciers. The difference between the median elevations of the two glacier types is not statistically significant, whereas the difference between their mean areas is statistically significant (4.87 km^2 for debris-covered glaciers and 0.42 km^2 for debris-free glaciers) (Table 1; Fig. 2).

Paul et al. (2013) demonstrated that debris-cover could lead to large interpretation differences (standard deviation of 6 % in area) by multi interpreters even if high resolution imageries such as QuickBird were used. We project an uncertainty of median elevation due to that of the area delineation by assuming that the area uncertainty exists solely in the lower half of debris-covered glaciers, at which the glacier boundary is often so unclear that cause misinterpretation. Considering the hypsometry and area statistic (Fig. 2 and Table 1), the area uncertainty in lower glaciers (±62 km^2, 6 % of total area of debris-covered glacier (1037 km^2) alters the median elevation by ±40 m, which results in area change of upper glaciers by 31 km^2. This uncertainty of median elevation is sufficiently small comparing with that of individual glaciers (±355 m).

The numbers and mean areas of debris-covered and debris-free glaciers are summarized by aspect, which is averaged over each individual glacier using ASTER GDEM2 images (Fig. 3). Larger numbers of debris-free glaciers face to the north and northwest, whereas directional preferences for debris-covered glaciers are uncertain (Fig. 3a). On the other hand, south- and north-facing debris-covered glaciers tend to be large, presumably because their sources are along the main east–west trending

Himalayan ridge, whereas such a relationship is not shown for debris-free glaciers (Fig. 3b). These aspect dependencies suggest that solar radiation controls the development of debris-free glaciers, and that the scale of a mountain ridge controls the expansion of a debris-covered glacier.

Histograms of total area, number, PMS slope area, and PMS slope ratio are summarized by glacier size (Fig. 4). Glaciers with sizes of 1.0–5.0 km^2 comprise the largest total glacier area in this region (debris-covered and debris-free glaciers combined; Fig. 4a). Area maxima in this size class are observed in several regions worldwide, such as in the Svartisen region, Norway (Paul and Andreassen, 2009), and the Tien Shan Mountains, Central Asia (Narama et al., 2010), whereas larger glaciers occupy larger areas in Greenland (Rastner et al., 2012). The largest area of debris-covered glaciers is comprised of glaciers with sizes of 10–50 km^2. The largest number of glaciers is in the size range of 0.1–0.5 km^2 (Fig. 4b). This trend is similar to glaciers located around Greenland (Rastner et al., 2012), in the Svartisen region, Norway (Paul and Andreassen, 2009), and on Baffin Island, Canada (Paul and Svoboda, 2010). The largest number of debris-covered glaciers is in the size range of 1.0–5.0 km^2. The largest area of PMS slopes is found in the basins of glaciers in the size range of 1.0–5.0 km^2 (debris-covered and debris-free glaciers combined; Fig. 4c). The PMS slope ratios of debris-covered glaciers exceed 2.5 for the smallest glaciers, and show a monotonically decreasing trend for larger glaciers (Fig. 4d). On the other hand, the PMS slope ratios of debris-free glaciers are less than 1.0, and no significant size-related trends are observed.

A histogram of the mean slope gradients of PMS slopes for debris-free and debris-covered glaciers is presented in Fig. 5; data were excluded for 379 debris-free glaciers with no adjacent PMS slopes, whereas PMS slopes were present around all debris-covered glaciers. The distribution of PMS slope gradients for both glacier types is normal, with peaks at gradients of 35–40° (average, 36.5°) for debris-covered glaciers and 25–30° for debris-free glaciers (average, 29.7°). A comparison of the mean PMS slope gradients shown in Table 1, which are calculated from the total merged PMS surfaces

TCD
8, 1305–1336, 2014

of debris-covered and debris-free glaciers in the region, shows that slope gradients are free of biases related to glacier size and topographic distinctions (i.e., gradients of debris-covered glaciers are steeper than those of debris-free glaciers.

Minimum elevations of glaciers (i.e., their terminus elevations) are plotted against their maximum elevations to compare the elevational distributions of debris-covered and debris-free glaciers (Fig. 6). For both glacier types, the mean minimum elevations, grouped in 200 m intervals of maximum elevation, show that the vertical range of glaciers (difference between the minimum and maximum elevations) correlates with the maximum elevation. That is, glaciers with large vertical ranges start at higher elevations. A comparison of the two glacier types at the same maximum elevation shows that the terminus elevations of debris-covered glaciers are substantially lower than those of debris-free glaciers. Furthermore, the termini of all glaciers starting from maximum elevations higher than 6800 m a.s.l. are debris covered.

4 Discussion

Our glacier inventory reveals that debris-covered glaciers exhibit larger areas, smaller numbers, and larger and steeper PMS slopes than debris-free glaciers in the Bhutan Himalaya (Figs. 4 and 5). In terms of glacier aspect, the dominant aspect of debris-free glaciers to the north and northwest suggests that their formation is controlled by solar radiation, while a notable number of debris-covered glaciers with north- and south-facing aspects suggest that their development is controlled by topographic factors, such as the sizes of PMS slopes (Fig. 3). The median elevation of debris-covered glaciers shows no significant difference from that of debris-free glaciers, although the elevational range of debris-covered glaciers is broader than that of debris-free glaciers (Fig. 2). On the other hand, debris-covered glaciers exhibit significantly lower terminus elevations than those of debris-free glaciers, given equal starting (maximum) elevations (Fig. 6). To understand these features, we examined the possible dependence of median elevation on annual precipitation (a climatic control) and PMS slope area (a topographic control). We further attempted to distinguish the influences of avalanche-fed accumulation and debris insulation on the median elevation, both of which are related to PMS slope areas and gradients.

4.1 Influence of precipitation

Ohmura et al. (1992) pointed out that the equilibrium line altitude (ELA) may be related to climatic factors, expressed in terms of summer mean temperature and annual precipitation, specifically, that the ELA might be lower in areas of increased precipitation (accumulation), and vice versa. In this study we assumed that latitudinal temperature gradients are negligible, as the target domain in this study is limited to 100 km in a S–N direction (Fig. 1); however, a S–N precipitation gradient should directly affect the ELA, for which median elevation is used as a proxy (Braithwaite and Raper, 2009). We obtained the spatial distribution of annual precipitation from TRMM 3B43 monthly data for the period 1998–2012 (Table S2). The median elevation of glacier area within the TRMM grid cell ($0.25^{\circ} \times 0.25^{\circ}$) tends to decrease with increasing annual precipitation, showing a weak negative correlation ($r = -0.33$; $p < 5\,\%$ in 36 grid cells) (Fig. 7a). Because topographic influences would be included in this plot, we further examined the influence of precipitation by limiting the analysis to glaciers with no PMS slopes ($n = 379$ in 32 grid cells). The plot still shows a similar weak negative correlation ($r = -0.34$; $p = 5.8\,\%$) (Fig. 7b). The results suggest that annual precipitation is a primary control on the median elevation of glaciers.

We further examined whether the relationships between annual precipitation and median elevation observed in Fig. 7 (-0.53 and $-0.61\,\mathrm{m\,mm^{-1}}$, for all glaciers and debris-free glaciers with no PMS slopes, respectively) are reasonable in the context of climatic influences on ELA. We estimated precipitation–air temperature gradients ($\mathrm{d}P/\mathrm{d}T$) from the regression lines in Fig. 7 ($\mathrm{d}z/\mathrm{d}P$), using a lapse rate ($\mathrm{d}T/\mathrm{d}z$) expressed as:

$$dP/dT = \frac{1}{(dz/dP)(dT/dz)}. \quad (1)$$

Assuming a lapse rate of $0.006 \pm 0.001\,^{\circ}\mathrm{C\,m^{-1}}$, precipitation–air temperature gradients are estimated to be 270–377 mm $^{\circ}\mathrm{C}^{-1}$ and 234–328 mm $^{\circ}\mathrm{C}^{-1}$, for all glaciers and debris-free glaciers with no PMS slopes, respectively. On the other hand, Ohmura et al. (1992) expressed precipitation as a function of temperature according to the polynomial

$$P = 645 + 296T + 9T^2 \quad (2)$$

and its differential

$$dP/dT = 296 + 18T \quad (3)$$

where T is the summer (June, July and August) mean air temperature. Applying the range of annual precipitation in the area (500–1000 mm), the summer mean air temperature and the precipitation–air temperature gradient are estimated to be −0.5 to 1.2 $^{\circ}\mathrm{C}^{-1}$ and 287–344 mm $^{\circ}\mathrm{C}^{-1}$, respectively. The estimated precipitation–air temperature gradient in the Bhutan Himalaya (234–377 mm $^{\circ}\mathrm{C}^{-1}$) covers the range of empirical values of ELAs worldwide (287–344 mm $^{\circ}\mathrm{C}^{-1}$). This result supports the assumption that the median elevation is an applicable proxy for the ELA, and that the median elevation is affected by precipitation even at regional scales in the Bhutan Himalaya. In this region, annual precipitation is affected by the Indian monsoon, under which precipitation is greater in the south than in the north (e.g., Eguchi, 1991). Thus, the distribution of median elevations suggests that glacier distributions in the Bhutan Himalaya are likely affected by the S–N precipitation gradient of the Indian monsoon.

TCD

8, 1305–1336, 2014

4.2 Influence of potential material-supply slopes

In addition to climatic constraints, topography also affects the location and extent of glaciers through debris supply and/or avalanche accumulation (Benn and Lehmkuhl, 2000; Scherler et al., 2011b). If PMS slopes supply sufficient snow to downslope glaciers, the effective accumulation rate should be significantly greater than that due strictly to precipitation. On the other hand, debris mantles can lower the median elevation by suppressing ice melting under the debris layer, and thus debris-covered ablation areas are expected to expand ice coverage relative to debris-free ice zones.

While features of PMS slopes vary markedly in a glacier system, we assume that PMS slopes should cause a deviation of the median elevation from the median elevation of glacier area within the TRMM grid cell ($0.25^{\circ} \times 0.25^{\circ}$) which is mainly determined by climatic factors (Fig. 7). The deviations of the median elevation show weak negative correlations with the PMS slope ratio (PMS slope area to glacier area) for both debris-covered ($r = -0.22$; $p = 1.3\,\%$) and debris-free ($r = -0.15$; $p < 0.1\,\%$) glaciers (Fig. 8a), suggesting that a larger PMS slope ratio lowers the median elevation of the glacier.

The steepnesses of PMS slopes are greater than those of glacier surfaces (Table 1), and they can be sufficiently steep to generate avalanches and rockfall (Fig. 5). In other words, gentle PMS slopes would effectively become a part of the glacier. The weak negative correlation observed between the PMS slope ratio and the median elevation (Fig. 8a) disappears when we combine the areas of the glacier body and its PMS slopes, and then examine the relationship of the combined area to the median elevation (Fig. 8b), suggesting that topographical influences are cancelled when PMS slopes are regarded as a part of the accumulation zone. In another words, the median elevation of the combined area is representative of the climate setting independent of the area of the PMS slopes.

4.3 Contributions of avalanches and debris to glaciers

To evaluate the degree to which the gradient or aspect of PMS slopes contributes to the negative correlation shown in Fig. 8a, the relationship between the deviation of the median elevation and the PMS slope ratio was examined, where PMS slopes are extracted according to their gradient (Fig. 9a) and aspect (Fig. 9b). Significant negative correlations are observed between deviations and slope gradients at slope gradients of ca. 30–40° for debris-free glaciers, which seems to correspond to their surface distributions, whereas negative correlations are observed at ca. 70–80° for debris-covered glaciers, a value which seems to be independent of their surface distribution (Fig. 9a). On the other hand, significant negative correlations are observed between deviations and aspects for PMS slopes facing south–southwest for debris-covered glaciers, whereas no significant correlation was observed for debris-free glaciers for any aspect (Fig. 9b). These results suggest that different processes contribute to the lowering of median elevations between the two glacier types.

The significant negative correlations observed at slope gradients of 30–40° for debris-free glaciers (Fig. 9a) are consistent with slope gradients at which high frequencies of avalanche are expected to occur (35–40°) (McClung and Schaerer, 1993). On the other hand, no obvious dependency is found in terms of slope aspect, although slight but very weak negative correlations are observed for north–northwest-facing PMS slopes (Fig. 9b). These results suggest that the influence of topography on the median elevation of individual debris-free glaciers is mainly caused by redistribution of snow accumulation from high to low elevations through avalanches.

Steep slopes of ca. 70–80° seem to correlate with a lowering of the median elevation of debris-covered glaciers, although the slope surfaces at such angles are small (Fig. 9a). In contrast, strong negative correlations are observed for south–southwest-facing PMS slopes (Fig. 9b), from which effective debris production is expected through diurnal freeze–thaw cycles (Nagai et al., 2013). This consistency strongly supports the

TCD
8, 1305–1336, 2014

hypothesis that debris supply is a cause of the lowering of the median elevations of debris-covered glaciers.

Field experimental investigations (Mattson et al., 1993) have revealed that thick debris cover prevents ice melting by an insulation effect. On the other hand, it has been pointed out that ice cliffs and ponds formed on heterogeneously rugged debris-covered surfaces effectively absorb heat and thus enhance the wastage of ice in debris-covered areas (Sakai et al., 2000, 2002). Several recent studies have also revealed a significant surface lowering of Himalayan debris-covered glaciers, the magnitudes of which are comparable to those of lowering in debris-free ablation zones (Kääb et al., 2012; Nuimura et al., 2011, 2012). In terms of the influence of area changes on the median elevation, however, the terminus position of heavily debris-covered glaciers are stable (Scherler et al., 2011a); however, debris-free glaciers in the Bhutan Himalaya have exhibited significant retreat rates in recent decades (Karma et al., 2003). Our statistical analyses reveal a significant relationship between the deviation of the median elevation and PMS slope aspects facing south–southwest, which is consistent with the slope aspect that contribute the most debris to glaciers (Nagai et al., 2013). On debris-covered glaciers, terminus location and thus median elevations appear stable during the retreat phase of glaciers (Scherler et al., 2011a); however, during the development phase of debris-covered glaciers in the Bhutan Himalaya, topographic influences are likely to lower the median elevation through insulation effects.

5 Conclusions

Climatic and topographic influences on the elevational distributions of glaciers in the Bhutan Himalaya were analysed and discussed using a new glacier inventory, together with an assessment of the areas of contiguous PMS slopes. Debris-covered glaciers exhibit larger areas, smaller numbers, and larger and steeper PMS slopes than those of debris-free glaciers (Table 1, Figs. 4 and 5). The median elevation of glaciers, which is used as a proxy for the ELA, shows significant negative correlations with annual

TCD
8, 1305–1336, 2014

precipitation, suggesting climatic influences on glacier distribution (Fig. 7). We found a weak but significant influence of topography on the elevation of glaciers, by comparing the deviation of the median elevation from the average in TRMM grid cells with the PMS slope ratio (defined as the PMS slope area divided by the glacier area) (Fig. 8a). When we integrated the PMS slopes into glacier area, the relationships disappeared (Fig. 8b). These observations suggest that PMS slopes cause deviations of glacier ELAs from regionally representative ELAs. Analyses of the dependency of the ELA on gradient and aspect suggest that PMS slopes influence the lowering of the median elevation through redistribution of snow accumulation by avalanches on debris-free glaciers, while debris-supply will enhance the expansion of ablation areas through the insulation effect of the debris layer, probably during the development phase of debris-covered glaciers (Fig. 9). An examination of the methodology employed herein, using PMS slopes in different climate regimes (such as the Karakorum), will contribute to further understandings and insights into the elevational distributions of glaciers in steep mountainous regions.

Supplementary material related to this article is available online at http://www.the-cryosphere-discuss.net/8/1305/2014/tcd-8-1305-2014-supplement.zip.

Acknowledgements. The ALOS data used in this study were provided by the project, "Study on Glacial Lake Outburst Floods in the Bhutan Himalayas", conducted under the Science and Technology Research Partnership for Sustainable Development (SATREPS), supported by the Japan Science and Technology Agency (JST) and the Japan International Cooperation Agency (JICA). This study was also supported by the Funding Program for Next Generation World-Leading Researchers (NEXT).

References

Arendt, A., Bolch, T., Cogley, J. G., Gardner, A., Hagen, J.-O., Hock, R., Kaser, G., Pfeffer, W. T., Moholdt, G., Paul, F., Radić, V., Andreassen, L., Bajracharya, S., Beedle, M., Berthier, E., Bhambri, R., Bliss, A., Brown, I., Burgess, E., Burgess, D., Cawkwell, F., Chinn, T., Copland, L., Davies, B., de Angelis, H., Dolgova, E., Filbert, K., Forester, R., Fountain, A., Frey, H., Giffen, B., Glasser, N., Gurney, S., Hagg, W., Hall, D., Haritashya, U. K., Hartmann, G., Helm, C., Herreid, S., Howat, I., Kapustin, G., Khromova, T., Kienholz, C., Koenig, M., Kohler, J., Kriegel, D., Kutuzov, S., Lavrentiev, I., LeBris, R., Lund, J., Manley, W., Mayer, C., Miles, E., Li, X., Menounos, B., Mercer, A., Mölg, N., Mool, P., Nosenko, G., Negrete, A., Nuth, C., Pettersson, R., Racoviteanu, A., Ranzi, R., Rastner, P., Rau, F., Rich, J., Rott, H., Schneider, C., Seliverstov, Y., Sharp, M., Sigurðsson, O., Stokes, C., Wheate, R., Winsvold, S., Wolken, G., Wyatt, F., and Zheltyhina, N.: Randolph Glacier Inventory version 3.2, digital media, available at: http://www.glims.org/RGI/RGI_Tech_Report_V3.2.pdf, last access: 20 February 2014, Global Land Ice Measurements from Space, Boulder Colorado, USA, 2012.

Basnett, S., Kulkarni, A. V., and Bolch, T.: The influence of debris cover and glacial lakes on the recession of glaciers in Sikkim Himalaya, India, J. Glaciol., 59, 1035–1046, doi:10.3189/2013JoG12J184, 2013.

Benn, D. I. and Lehmkuhl, F.: Mass balance and equilibrium-line altitudes of glaciers in high-mountain environments, Quatern. Int., 65, 15–29, doi:10.1016/S1040-6182(99)00034-8, 2000.

Braithwaite, R. J. and Raper, S. C. B.: Estimating equilibrium-line altitude (ELA) from glacier inventory data, Ann. Glaciol., 50, 127–132, doi:10.3189/172756410790595930, 2009.

Bolch, T., Kulkarni, A., Kääb, A., Huggel, C., Paul, F., Cogley, J. G., Frey, H., Kargel, J. S., Fujita, K., Scheel, M., Bajracharya, S., and Stoffel, M.: The state and fate of Himalayan glaciers, Science, 336, 310–314, doi:10.1126/science.1215828, 2012.

Eguchi, T.: Regional and Temporal Variations in Precipitation in the Eastern Part of the Himalayas, Kochi, Japan, Faculty of Humanities and Economics, Kochi University, 1991.

Frey, H., Paul, F., and Strozzi, T.: Compilation of a glacier inventory for the western Himalaya from satellite data: methods, challenges and results, Remote Sens. Environ., 124, 832–843, doi:10.1016/j.rse.2012.06.020, 2012.

Fujita, K.: Effect of precipitation seasonality on climatic sensitivity of glacier mass balance, Earth Planet. Sc. Lett., 276, 14–19, doi:10.1016/j.epsl.2008.08.028, 2008.
Fujita, K. and Nuimura, T.: Spatially heterogeneous wastage of Himalayan glaciers, P. Natl. Acad. Sci. USA, 108, 14011–14014, doi:10.1073/pnas.1106242108, 2011.
Fujita, K., Suzuki, R., Nuimura, T., and Sakai, A.: Performance of ASTER and SRTM DEMs, and their potential for assessing glacial lakes in the Lunana region, Bhutan Himalaya, J. Glaciol., 54, 220–228, doi:10.3189/002214308784886162, 2008.
Gardelle, J., Berthier, E., Arnaud, Y., and Kääb, A.: Region-wide glacier mass balances over the Pamir-Karakoram-Himalaya during 1999–2011, The Cryosphere, 7, 1263–1286, doi:10.5194/tc-7-1263-2013, 2013.
Hayakawa, T. S., Oguchi, T., and Lin, Z.: Comparison of new and existing global digital elevation models: ASTER G-DEM and SRTM-3, Geophys. Res. Lett., 35, L17404, doi:10.1029/2008GL035036, 2008.
Hewitt, K.: Glacier change, concentration, and elevation effects in the Karakoram Himalaya, upper Indus basin, Mt. Res. Dev., 31, 188–200, doi:10.1659/MRD-JOURNAL-D-11-00020.1, 2011.
Huffman, G. J., Bolton, D. T., Neilkin, E. J., and Wolff, D. B.: The TRMM multi satellite precipitation analysis (TMPA): quasi-global, multiyear, combined-sensor precipitation estimates at fine scales, J. Hydrometeorol., 8, 38–55, doi:10.1111/j.1541-0064.1968.tb00567.x, 2007.
Immerzeel, W. W., van Beek, L. P. H., and Bierkens, M. F. P.: Climate change will affect the Asian water towers, Science, 328, 1382–1385, doi:10.1126/science.1183188, 2010.
Iwata, S., Aoki, T., Kadota, T., Seko, K., and Yamaguchi, S.: Morphological evolution of debris cover on Khumbu Glacier, in: Debris-Covered Glaciers, edited by: Nakawo, M., Raymond, C. F., and Fountain, A., IAHS Publ., 264, 3–11, 2000.
Kääb, A.: Combination of SRTM3 and repeat ASTER data for deriving alpine glacier flow velocities in the Bhutan Himalaya, Remote Sens. Environ., 94, 463–474, doi:10.1016/j.rse.2004.11.003, 2005.
Kääb, A., Berthier, E., Nuth, C., Gardelle, J., and Arnaud, Y.: Contrasting patterns of early twenty-first-century glacier mass change in the Himalayas, Nature, 488, 495–498, doi:10.1038/nature11324, 2012.
Karma, Y. A., Naito, N., Iwata, S., and Yabuki, H.: Glacier distribution in the Himalayas and glacier shrinkage from 1963 to 1993 in the Bhutan Himalayas, Bull. Glaciol. Res., 20, 29–40, 2003.

Kaser, G., Cogley, J. G., Dyurgerov, M. B., Meier, M. F., and Ohmura, A.: Mass balance of glaciers and ice caps: consensus estimates for 1961–2004, Geophys. Res. Lett., 33, L19501, doi:10.1029/2006GL027511, 2006.

Kaser, G., Großhauser, M., and Marzeion, B.: Contribution potential of glaciers to water availability in different climate regimes, P. Natl. Acad. Sci. USA, 107, 20223–20227, doi:10.1073/pnas.1008162107, 2010.

Mattson, L. E., Gardner, J. S., and Young, G. J.: Ablation on debris covered glaciers: an example from the Rakhiot Glacier, Punjab, Himalaya, in: Snow and Glacier Hydrology, edited by: Young, G. J., IAHS Publ., 218, 289–296, 1993.

McClung, D. M. and Schaerer, P. A.: The Avalanche Handbook, The Mountaineers, Seattle, WA, 272 pp., 1993.

Mool, P. K., Wangda, D., Bajracharya, S. R., Kunzang, K., Gurung, D. R., and Joshi, S. P.: Inventory of Glaciers, Glacial Lakes and Glacial Lake Outburst Floods, Bhutan, ICIMOD, Kathmandu, Nepal, 227 pp., 2001.

Nagai, H., Fujita, K., Nuimura, T., and Sakai, A.: Southwest-facing slopes control the formation of debris-covered glaciers in the Bhutan Himalaya, The Cryosphere, 7, 1303–1314, doi:10.5194/tc-7-1303-2013, 2013.

Narama, C., Kääb, A., Duishonakunov, M., and Abdrakhmatov, K.: Spatial variability of recent glacier area changes in the Tien Shan Mountains, Central Asia, using Corona (~ 1970), Landsat (~ 2000), and ALOS (~ 2007) satellite data, Global Planet. Change, 71, 42–54, doi:10.1016/j.gloplacha.2009.08.002, 2010.

Nuimura, T., Fujita, K., Fukui, K., Asahi, K., Aryal, R., and Ageta, T.: Temporal changes in elevation of the debris-covered ablation area of Khumbu glacier in the Nepal Himalaya since 1978, Arct. Antarct. Alp. Res., 43, 246–255, doi:10.1657/1938-4246-43.2.246, 2011.

Nuimura, T., Fujita, K., Yamaguchi, S., and Sharma, R. R.: Elevation changes of glaciers revealed by multitemporal digital elevation models calibrated by GPS survey in the Khumbu region, Nepal Himalaya, 1992–2008, J. Glaciol., 58, 648–656, doi:10.3189/2012JoG11J061, 2012.

Ohmura, A., Kasser, P., and Funk, M.: Climate at the equilibrium line of glaciers, J. Glaciol., 38, 397–411, 1992.

Paul, F. and Andreassen, L. M.: A new glacier inventory for the Svartisen region, Norway, from Landsat ETM+ data: challenges and change assessment, J. Glaciol., 55, 607–618, doi:10.3189/002214309789471003, 2009.

Paul, F. and Svoboda, F.: A new glacier inventory on southern Baffin Island, Canada, from ASTER data: II. Data analysis, glacier change and applications, J. Glaciol., 53, 22–31, doi:10.3189/172756410790595921, 2010.
Paul, F., Barrand, N. E., Baumann, S., Berthier, E., Bolch, T., Casey, K., Frey, H., Joshi, S. P., Konovalov, V., Le Bris, R., Mölg, N., Nosenko, G., Nuth, C., Pope, A., Racoviteanu, A., Rastner, P., Raup, B., Scharrer, K., Steffen, S., and Winsvold, S.: On the accuracy of glacier outlines derived from remote-sensing data, Ann. Glaciol., 54, 171–182, doi:10.3189/2013AoG63A296, 2013.
Pfeffer, W. T., Arendt, A. A., Bliss, A., Bolch, T., Cogley, J. G., Gardner, A. S., Hagen, J., Hock, R., Kaser, G., Kienholz, C., Miles, E. S., Moholdt, G., Mölg, N., Paul, F., Radić, V., Rastner, P., Raup, B. H., Rich, J., Sharp, M. J., and the Randolph Consortium: The Randolph Glacier Inventory: a globally complete inventory of glaciers, J. Glaciol., accepted, 2014.
Radić, V. and Hock, R.: Regionally differentiated contribution of mountain glaciers and ice caps to future sea-level rise, Nat. Geosci., 4, 91–94, doi:10.1038/ngeo1052, 2011.
Raper, S. C. B. and Braithwaite, R. J.: Low sea level rise projections from mountain glacier and icecaps under global warming, Nature, 439, 311–313, doi:10.1038/nature04448, 2006.
Rastner, P., Bolch, T., Mölg, N., Machguth, H., Le Bris, R., and Paul, F.: The first complete inventory of the local glaciers and ice caps on Greenland, The Cryosphere, 6, 1483–1495, doi:10.5194/tc-6-1483-2012, 2012.
Raup, B. and Khalsa, S. J. S.: GLIMS analysis tutorial, Boulder, CO, University of Colorado, National Snow and Ice Data Center, available at: http://www.glims.org/MapsAndDocs/guides.html (last access: 1 September 2013), 2007.
Sakai, A., Takeuchi, N., Fujita, K., and Nakawo, M.: Role of supraglacial ponds in the ablation process of a debris-covered glacier in the Nepal Himalayas, in: Debris-Covered Glaciers, edited by: Nakawo, M., Raymond, C. F., and Fountain, A., IAHS Publ., 265, 119–130, 2000.
Sakai, A., Nakawo, M., and Fujita, K.: Distribution characteristics and energy balance of ice cliffs on debris-covered glaciers, Nepal Himalaya, Arct. Antarct. Alp. Res., 34, 12–19, 2002.
Scherler, D., Bookhagen, B., and Strecker, M. R.: Spatially variable response of Himalayan glaciers to climate change affected by debris cover, Nat. Geosci., 4, 156–159, doi:10.1038/ngeo1068, 2011a.
Scherler, D., Bookhagen, B., and Strecker, M. R.: Hillslopeglacier coupling: the interplay of topography and glacial dynamics in High Asia, J. Geophys. Res., 116, F02019, doi:10.1029/2010JF001751, 2011b.

TCD
8, 1305–1336, 2014

Climatic and topographic influences on glacier distribution

H. Nagai et al.

Tachikawa, T., Hato, M., Kaku, M., and Iwasaki, A.: The characteristics of ASTER GDEM version 2, Proc. IGARSS 2011 Symposium, Vancouver, Canada, 24–29 July 2011, 3657–3660, 2011.
Tadono, T., Kawamoto, S., Narama, C., Yamanokuchi, T., Ukita, J., Tomiyama, N., and Yabuki, H.: Development and validation of new glacial lake inventory in the Bhutan Himalayas using ALOS "Daichi", Global Environ. Res., 16, 31–40, 2012.
Toutin, T.: Three-dimensional topographic mapping with ASTER stereo data in rugged topography, IEEE T. Geosci. Remote, 40, 2241–2247, doi:10.1109/TGRS.2002.802878, 2002.
Yamamoto, M. K., Ueno, K., and Nakamura, K.: Comparison of satellite precipitation products with rain gauge data for the Khumbu region, Nepal Himalaya, J. Meteorol. Soc. Jpn., 89, 597–610, doi:10.2151/jmsj.2011-601, 2011.
Yao, T., Thompson, L., Yang, W., Yu, W., Gao, Y., Guo, X., Yang, X., Duan, K., Zhao, H., Xu, B., Pu, J., Lu, A., Xiang, Y. Kattel, D. B., and Joswiak, D.: Different glacier status with atmospheric circulations in Tibetan Plateau and surroundings, Nature Clim. Change, 2, 663–667, doi:10.1038/nclimate1580, 2012.

TCD
8, 1305–1336, 2014

Table 1. Statistical summary of glaciers in the Bhutan Himalaya. Glacier area is the projected horizontal area. The debris-covered area of a glacier contributes to glacier area while adjacent PMS slopes are not included in the glacier area. The PMS slope ratio is the PMS slope area divided by the mean glacier area.

		Debris-covered glaciers	Debris-free glaciers
Number		213	1366
Total area (km^2)	Glaciers	1037.3	570.2
	PMS slopes	908.8	194.1
	Debris-covered areas	208.9	–
Mean area (km^2)	Glaciers	4.87	0.42
	PMS slopes	4.27	0.14
	Debris-covered areas	0.98	–
PMS slope ratio		1.05	0.47
Elevation of glaciers (m a.s.l.)	Maximum	7506	6799
	Minimum	4021	4662
	Mean	5631	5537
	Median	5537	5495
Mean gradient (°)	Glacier surfaces	19.2	22.1
	PMS slopes	37.1	33.4

TCD
8, 1305–1336, 2014

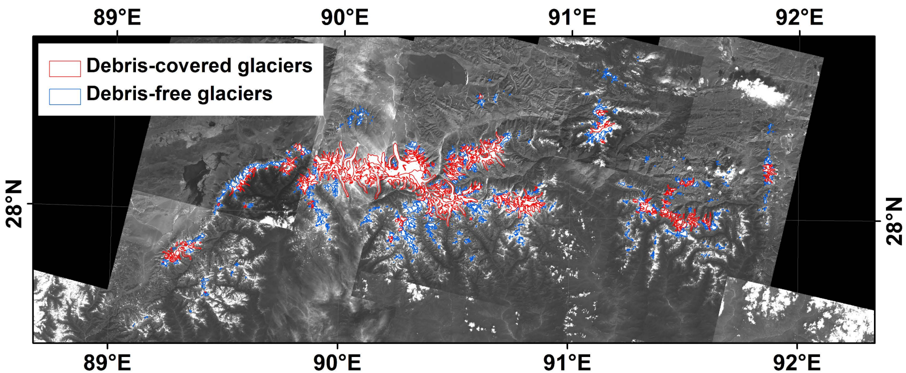

Fig. 1. Glacier distribution in the Bhutan Himalaya. Image is a mosaic of AVNIR-2 images (band 3).

TCD
8, 1305–1336, 2014

Climatic and topographic influences on glacier distribution

H. Nagai et al.

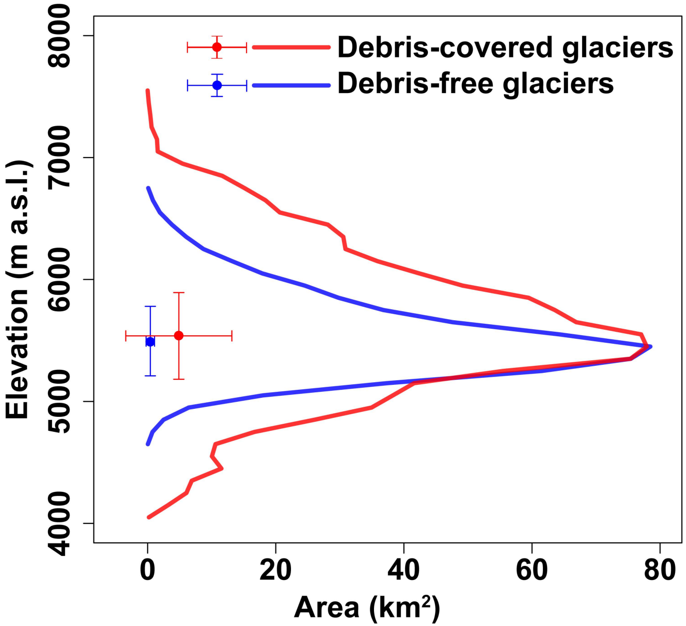

Fig. 2. Hypsometries of debris-covered and debris-free glaciers in the Bhutan Himalaya, summarized in 100 m elevation bins. The points with error bars show the mean values of individual median elevations.

TCD
8, 1305–1336, 2014

Climatic and topographic influences on glacier distribution

H. Nagai et al.

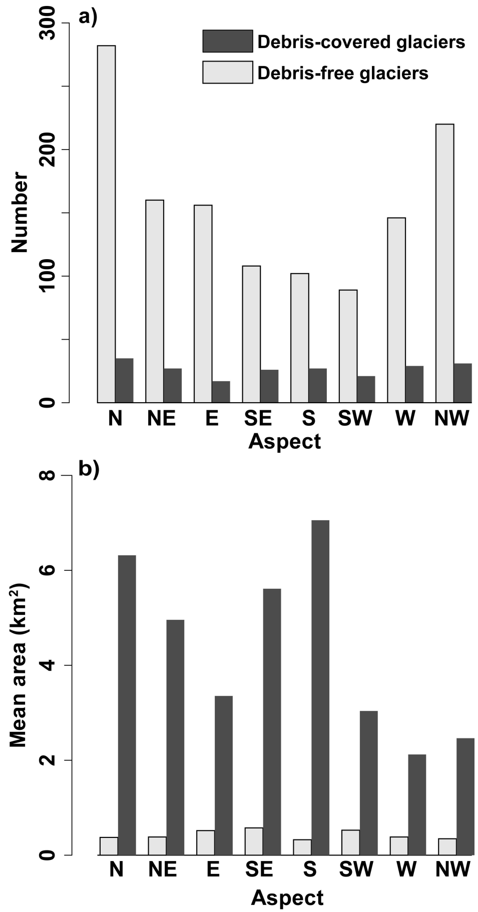

Fig. 3. Histograms of the number **(a)** and the mean area **(b)** of glaciers in the Bhutan Himalaya at eight different aspects.

TCD
8, 1305–1336, 2014

Climatic and topographic influences on glacier distribution

H. Nagai et al.

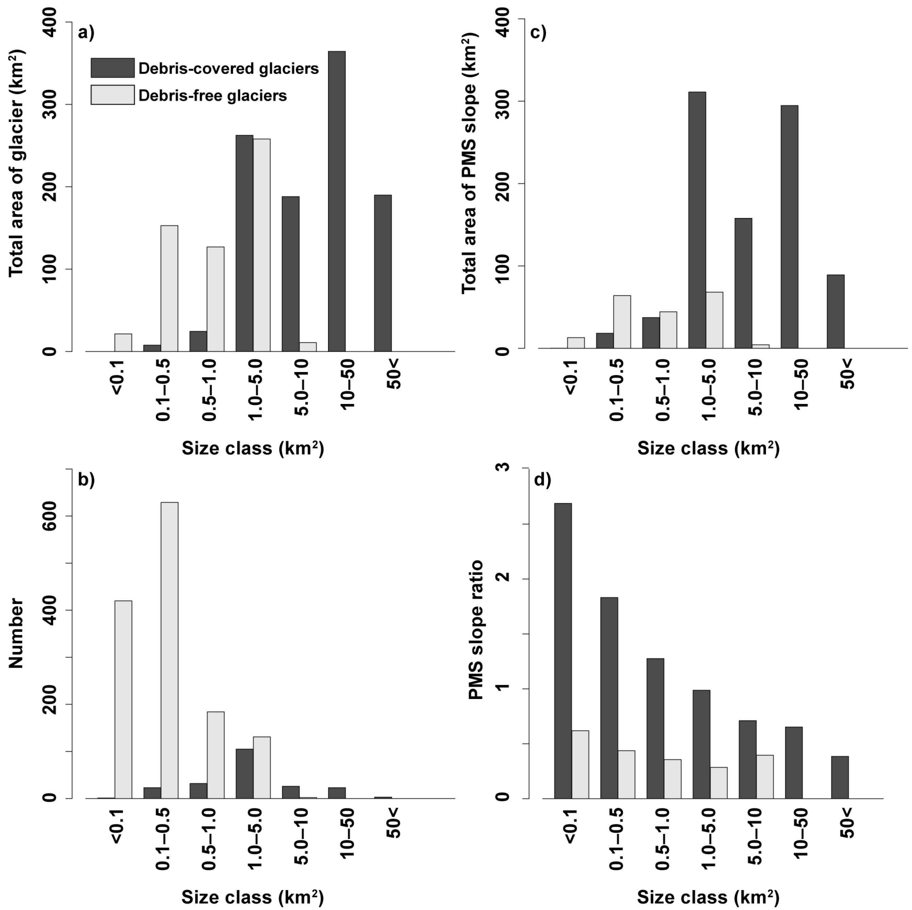

Fig. 4. Histograms of **(a)** total area, **(b)** number, **(c)** potential material-supply (PMS) slope area, and **(d)** PMS slope ratio of glaciers in the Bhutan Himalaya, summarized by glacier size (area).

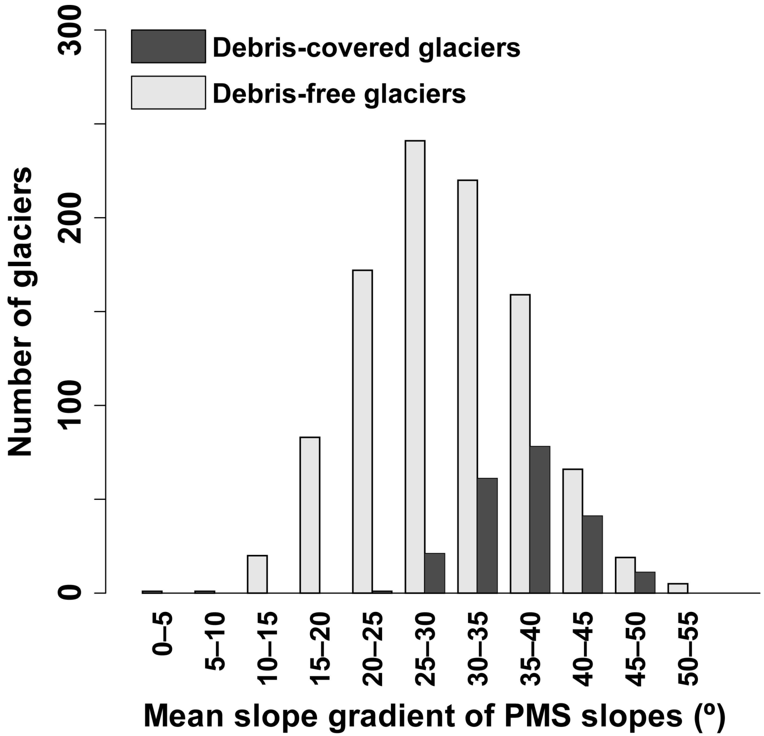

Fig. 5. Number of debris-covered and debris-free glaciers summarized by mean slope gradient of their potential material-supply (PMS) slope in the Bhutan Himalaya. Debris-free glaciers having no PMS slope are excluded ($n = 379$).

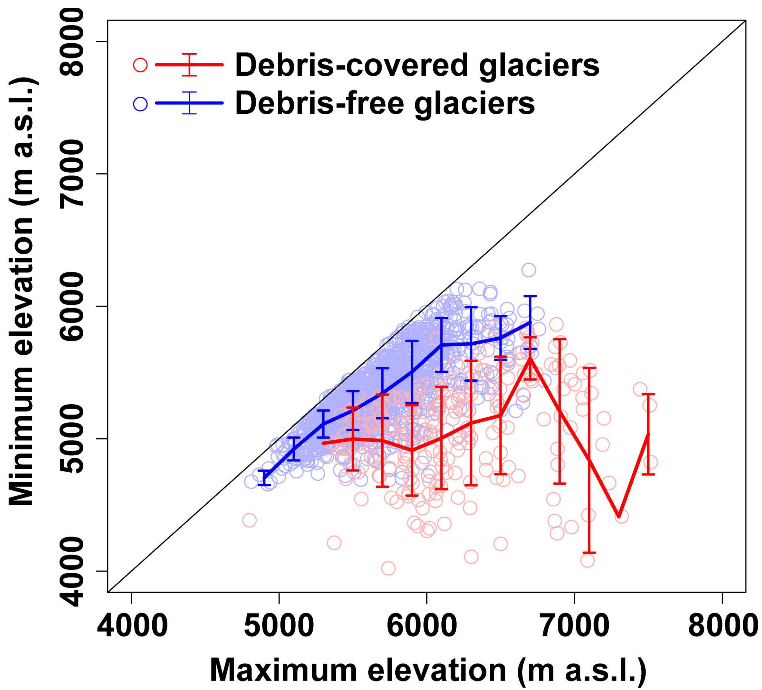

Fig. 6. Minimum vs. maximum elevations of glaciers in the Bhutan Himalaya. The mean and standard deviation are given for maximum elevations grouped in 200 m intervals (shown as lines with bars).

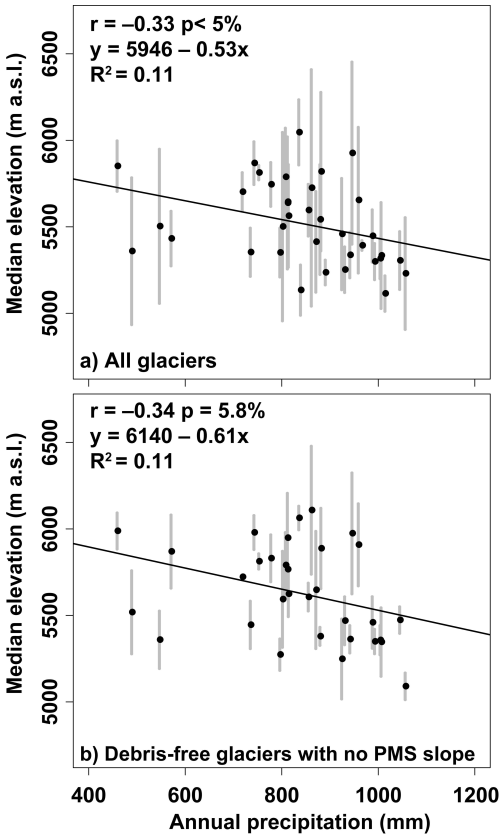

Fig. 7. Relationships between median elevation and annual precipitation for **(a)** all glaciers, and **(b)** debris-free glaciers with no potential material-supply (PMS) slopes, in the Bhutan Himalaya. The parameters are averaged in TRMM 3B43 grid cells (0.25° × 0.25°).

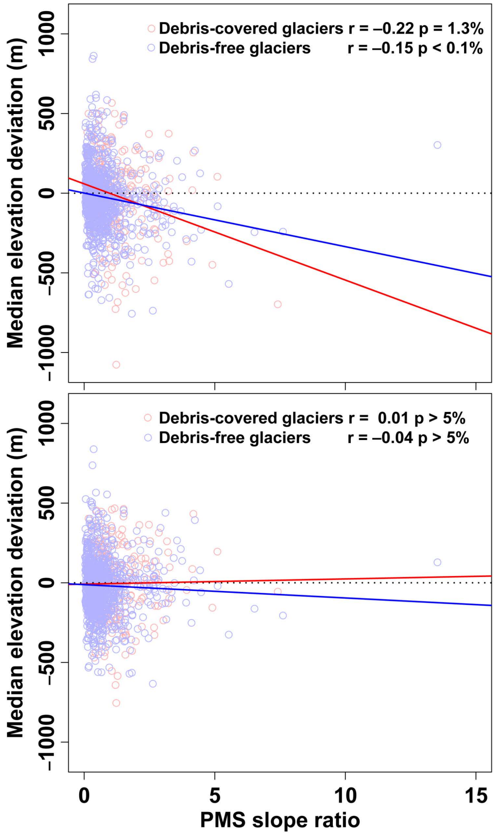

Fig. 8. Deviation of the median elevation plotted against the potential material-supply (PMS) slope ratio of glaciers in the Bhutan Himalaya, expressed using **(a)** glacier area and **(b)** a summation of glacier and PMS slope areas. The deviation is defined as the difference from the median elevation of glacier area within the TRMM grid cell (0.25° × 0.25°).

TCD
8, 1305–1336, 2014

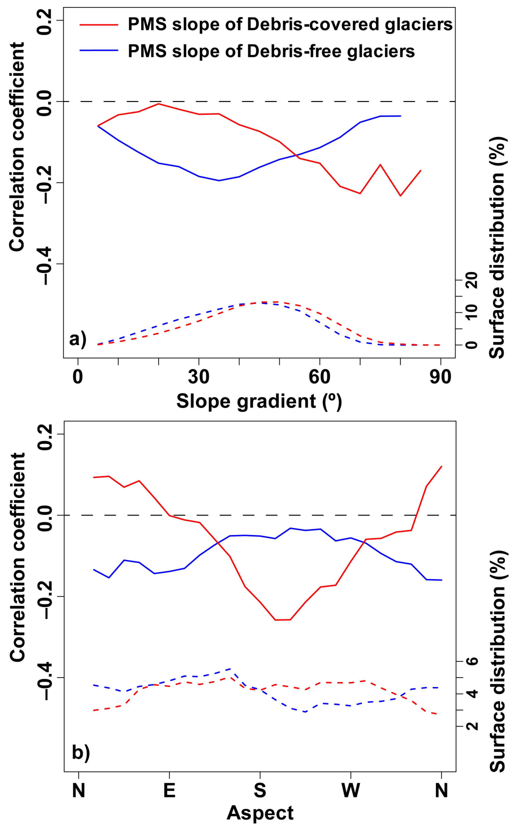

Fig. 9. Correlation coefficients representing the deviation of the median elevation and the potential material-supply (PMS) slope ratio of debris-covered and debris-free glaciers in the Bhutan Himalaya, by **(a)** gradients, in 5° bins, and **(b)** aspect, in 15° bins. Also shown are the distributions of PMS slopes, in percent.

TCD
8, 1305–1336, 2014

Climatic and topographic influences on glacier distribution

H. Nagai et al.